MEASURES OF NON-LINEARITY IN AIR TEMPERATURE SEQUENCE OVER MICHIGAN GREAT LAKE

Sabbir Reza Tarafdar[1], Kalpana Roy[2], Tushnik Sarkar[3*], Santanu Thandar[4], and Khondekar Mofazzal Hossain[5]
*Department of Electrical Engineering
Dr. B. C. Roy Engineering College, Durgapur – 713206. West Bengal, India.
Email id – sabbir.tarafdar@bcrec.ac.in

Abstract: ***The level of nonlinearity in the dynamics of the daily mean air temperature data series over Michigan Grate Lake has been examined using appropriate statistical tools. The time series is collected from the database of Tides and Currents under the National Oceanic and Atmospheric Administration (NOAA), Menominee, MI, Station ID: 9087088, length 1584 days from 14th March, 2011 to 14th July, 2015 for this purpose. The raw data has been pre-processed using simple exponential smoothing and discrete wavelet transform (DWT) based denoising. To gauge the extent of nonlinearity under the dynamics of the test series, delay vector variance (DVV) strategy is applied. The study yields that the fluctuation of daily mean air temperature over Michigan Great Lake poses deterministic, regular, non-linear behaviour in the temporal domain.***

Key words: ***Michigan Great Lake, Lake surface temperature time series, Simple exponential smoothing, Discrete wavelet transform, Delay vector variance***

1. INTRODUCTION

For atmospheric research communities, it is obvious to investigate and forecast the dynamic characteristics of an ever-changing ambience, and it is a very ancient practice. Some of the crucial parameters that have a substantial influence on climate change are dew-point, rainfall, atmospheric pressure, air temperature, wind speed, [1] [2], ozone abundance [3], etc. Current researchers aim to explore the dynamic behaviour of daily mean temperature over the Michigan Great Lake (Fig.1) in this work. The dynamic behaviours of the air temperature over the Lake play a fundamental role in comprehending the Lake's overall health and its surroundings.

The temperature data series for this investigation is considered for 14th March 2011 to 14th July 2015 (Tides and Currents under National Oceanic and Atmospheric Administration, Station ID: 9087088, https://tidesandcurrents.noaa.gov/). The duration mentioned above is picked for the present study due to its longest available span without missing data. The missing data demands interpolation in the data series, may be leading to ambiguous conclusions. Michigan Great lake is the largest Lake entirely within one country, i.e. United States of America (USA), by surface area (58,026 km2), coordinated by 44°N, 87°W. The Lake is shared by the states of Illinois, Indiana, Michigan, and Wisconsin from west to east.

Around twelve million people bordering Lake Michigan, mainly Chicago and Milwaukee metropolitan areas, directly depend on the Michigan Great Lake for their drinking water [4]. The Lake has immense commercial and societal prominence in the diverse sectors, i.e., steel industry, shipping, commercial fisheries [5], tourism, etc., on its shore. It is inevitable to mention that Lake Michigan has a mammoth geo-biologic and socio-economic significance [4]. Due to the effect of these pollutants on the Lake, as discussed earlier, the critical meteorological parameter around the Lake, like temperature, water level, wind speed, salinity, conductivity, etc., may get influenced and

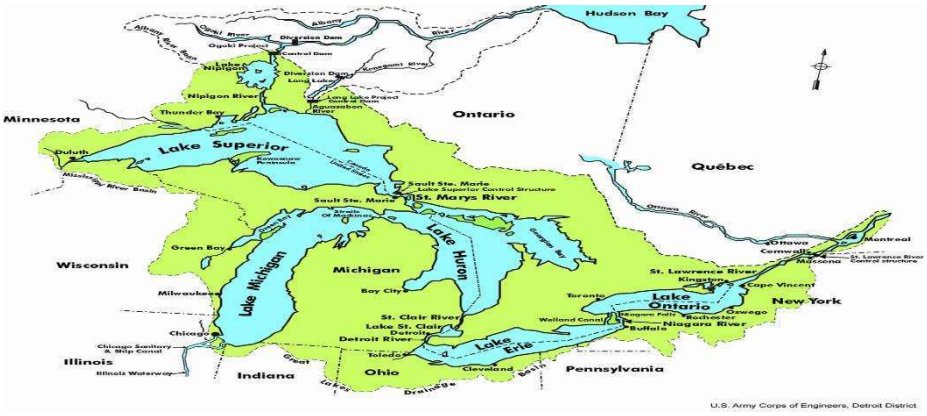

Figure 1: Michigan Great Lake (1200px-Great_Lakes_1.PNG (1200×994) (wikimedia.org))

Some of the pertinent, similar literatures includes: temperature data analysis on Ontario Lake basins by S. I. Ahmed et.al [6], water temperature research of the Gate lakes by Brenda M. L. et.al [7], study of Vincent Y. S. C. et. al regarding water label fluctuations of Lake Huron – Michigan [7], the work of Frank H Quinn et.al on air temperature and precipitation data over six great lakes [8], exploring the relation between snow falls and temperature on Michigan Lake region by Craig A. Clark [9] etc. Whereas Robert J. Ruhf carried an statistical analysis on precipitation data [10], Cynthia E. Sellinger took evaporation , temperature and precipitation sequences and obtained interrelations [11], Navid et al. studied on wind data [12] etc. The current study intends to explore the dynamics of temperature fluctuations over the Michigan Great Lake, as a lack of such findings is evident from the literature survey.

The time-series data obtained from measuring instruments are often contaminated with spurious noises that should be reduced to a certain extent by signal preprocessing techniques to avoid indistinct inferences. In the present study, the signal is pre-processed by the Simple Exponential Smoothing (SES) technique [13] and DWT denoising technique [14] [15]. Gauge the degree of non–linearity in the fluctuation of temperature, popular tool DVV analysis has been employed [16] [17] [18]. The advantage of the DVV method over other methods is illustrated in the literature [19].

The outcomes of the investigation yield that the fluctuation of daily mean air temperature over Michigan Great Lake poses a non-linear, deterministic, regular behaviour with respect to time. Identification of the dynamic structure will contribute to climate-logical-forecasting & choice-making regarding numerous yearly basis public welfare ventures of the location.

II. THEORY

The theoretical foundation of the applied methods in the current study is elucidated in this section.

Simple Exponential Smoothing Time series data is often smoothed by the simple exponential smoothing [13] technique. This technique assigns past observations by exponentially decaying weighted factors to estimate future values. If the raw data sequence is denoted by $\{x_i\}$ then, $\{y_i\}$ is the output of the exponential smoothing method. Considering $t = 0$ is the starting point of the sequence of observations, then the simplest form of exponential smoothing can be represented by

$$y_0 = x_0$$
$$y_i = \rho x_{i-1} + (1-\rho) y_{i-1} \qquad 0 < \rho < 1 \tag{1}$$

where, y_i and ρ represent the smoothed data series and smoothing constant respectively. ρ lies between 0 to 1 [20]. Choice of ρ close to the right-hand neighbourhood of 0.5 often provides effective smoothing [21]. In this work, the value of ρ is chosen as 0.51.

2.1 Denoising by Discrete Wavelet Transform (DWT)

To improve the accuracy of information hidden within the data series, it is obligatory to de-noise the signal from the interfering white noises coming from several sources. Though lots of denoising techniques are available, Discrete Wavelet Transforms (DWT) [14] [15] based denoising is used in this work. DWT based approach suits well, both for stationary and non-stationary signals. A signal is said to be stationary when its frequency contents remain unchanged over time, whereas the presence of time-dependent frequencies makes the signal non-stationarity. As most of the natural signals are non-stationary, the signal under investigation in this work is also assumed to be non-stationary. There are three consecutive steps in this method, i.e. (a) signal decomposition, (b) thresholding of DWT coefficients, and (c)signal reconstruction [22]. The DWT coefficients measure the degree of resemblance between the wavelet and signal frequencies. When the test signal is convoluted with the scaled wavelet DWT coefficient is generated. Scaled wavelets possess a band-pass spectrum. Let D be the real-valued data series. Then, the mother wavelet is denoted as an orthogonal operator ξ then the DWT is computed by

$$L = \xi D \tag{2}$$

where, L indicates the wavelet transformed matrix of the data D. Wavelet coefficients $l_{r,c}$ are the elements L [23]. In DWT denoising two most important tasks are (a) adoption of appropriate mother wavelet and (b) rejection of inconsiderable elements. The rejection of insignificant components is made by thresholding, soft or hard [24].

2.2 Selection of the mother wavelet

An ample number of mother wavelets (orthogonal bases) [14] [15] are present to compute DWT based denoising. The appropriate mother wavelet is selected by minimising the entropy of the wavelet transformed data matrix [25] [26]. The energy is misbalanced by the WT. The best WT possesses the most energy misbalance. The minimum entropy corresponds to the highest ratio of bigger coefficients to many smaller coefficients. For each mother wavelet, an entropy score is figured out. The mother wavelet having best the entropy score is selected for the de-nosing process. The growing coefficients of Daubechies, Symmlet, and Coiflet wavelet along with the Harr wavelet [15] are the members of the mother wavelet library. Shannon entropy [25], which provides the most adaptive measure, is given by

$$S(L) = -\sum_{r,c} l'_{r,c} \log l'_{r,c} \tag{3}$$

here $l'_{r,c}$ is given by

$$l'_{r,c} = \left| l_{r,c} \right| \Big/ \sum \left| l_{r,c} \right| \tag{4}$$

The various $S(L)$ for different mother wavelets applied to daily mean air temperature data of Menominee, MI, USA (Stations Code: 9087088) are shown in Fig.2.

2.3 Thresholding of DWT coefficients

Insignificant DWT coefficients are rejected by thresholding [23] operation. However, important information is kept intact. Thresholding can be either (i) hard or (ii) soft.

Hard thresholding is defined as:

$$I_{r,c} = \begin{cases} 0 & |I_{r,c}| < \lambda \\ I_{r,c} & |I_{r,c}| \geq \lambda \end{cases} \quad (5)$$

on the other hand, soft thresholding is defined as

$$I_{r,c} = sign(I_{r,c})(|I_{r,c}| - \lambda) \quad (6)$$

where, $I_{r,c}$ is DWT coefficients and λ is a certain threshold value.

The DWT coefficients produced from the largest scales of the wavelets are not thresholded irrespective of their size λ. The value of threshold δ is estimated by the method of Donoho [23] [27] as:

$$\lambda = \sigma\sqrt{\log N} \quad (7)$$

where, the number of signal samples is N and σ is the standard deviation of DWT coefficients.

The de-noised signal is obtained from the thresholded DWT coefficients applying inverse discrete wavelet transform (IDWT). IDWT is the reverse process of DWT decomposition.

[28]. The decomposition and reconstruction filters are identical, except that they are in the reverse time frame.

2.4. Delay vector variance method (DVV)

In DVV method, d - dimensional phase space is formed from the time-series sequence considering delay vectors (DV) with embedding time delay τ. The delay vectors are represented as

$$x(a) = [x_{a-d\tau}, ..., x_{a-\tau}]_{\text{here,}}\ a = 1, 2, ..., N \quad (8)$$

DVs, within the Euclidean distance r_d from the $x(a)$, are grouped as $\lambda_a(r_d)$. For each set of λ_a, σ^{*2}, an unpredictability measure is evaluated at a given embedding dimension d. The embedding dimension d, which yields the least target variance σ^{*2}, is taken as the optimum one. The varying standardised distances examine the whole range of pair wise distances [17].

2.5. Algorithm for Delay Vector Variance (DVV) Method

The Euclidean distances between each and every pair of DVs are calculated as follows:

$$d(r, c) = \|x(r) - x(c)\| \quad (r \neq c) \quad (9)$$

μ_d and σ_d are the mean and standard deviation of $d(r, c)$. The $\lambda_a(r_d)$ is a set of DVs which lies in the close vicinity of the delay vector $x(a)$ expressed as-

$$\lambda_a(r_d)=\{x(i)\ \ \|x(a)-x(i)\|\le r_d\} \quad (10)$$

Let, $\sigma_a^2(r_d)$ is the variance for each group of $\lambda_a(r_d)$. The target variance $\sigma^{*2}(r_d)$ is evaluated by normalising (with the variance of the original test signal (σ_x^2) the average variances of all sets $\lambda_a(r_d)$ in Eq.10.

$$\sigma^{*2}(r_d)=\frac{\left(\frac{1}{N}\right)\sum_{a=1}^{N}\sigma_a^2(r_d)}{\sigma_x^2} \quad (11)$$

For a valid variance measurement, it is desired to have minimum 30 DVs (smallest set size) in a group [29], otherwise, the result may be misleading. The distance axis is standardised by putting $\frac{r_d-\mu_d}{\sigma_d}$ in place of r_d . The mean and variances of that standardized distance are zero and unity, respectively.

Target variance $\sigma^{*2}(r_d)$ which is the function of standardized distance is depicted as "DVV plot". The minimum target variance $\sigma_{\min}^{*2}=\min_{r_d}[\sigma^{*2}(r_d)]$ is the degree of noise within the data series. The extent of noise is the dominance of the stochastic part. The incidence of strong deterministic nature will cause small target variance for tiny spans.

As the standardized distance increases, more and more DVs come into a single universal group, and the variance of the targets reaches towards the variance of the test series. Eventually, the DVV plot converges to unity at the furthest right of the graph.

Iterative amplitude adjusted Fourier transform (IAAFT) [30]has been applied to build surrogate time series. DVV scatter diagram is developed from the original and the surrogate time series. In the scatter diagram, the horizontal axis indicates the target variance of the original signal and the vertical for the surrogated data series.

In the plot, for a linear time series DVV scatter diagram coincides with the bisector line. Contrary, DVV Scatter diagram deviates from the line of bisection for a non-linear series. Root mean square error (RMSE) has been computed between the σ^{*2} s of the original signal and the averaged σ^{*2} s of all the surrogate sequence. RMSE works as a quantifier of the degree of nonlinearity.

$$RMSE=\sqrt{\left\langle\left(\sigma^{*2}(r_d)-\frac{\sum_{i=1}^{N}\sigma_{s,i}^{*2}(r_d)}{N_s}\right)^2\right\rangle} \quad (12)$$

With span r_d, $\sigma_{s,i}^{*2}(r_d)$ indicates target variance of the i^{th} surrogate & a mean is considered for all spans r_d which are effective in each and every surrogate & DVV plots.

III. RESULTS

Figure 2 denotes the raw signal of the daily mean air temperature of the Michigan Great Lake from 14th March 2011 to 14th July 2015. The exponentially smoothed data sequence is shown in the figure. 3. Random noise is removed by DWT denoising. For this purpose, the mother wavelet that yields the minimum entropy value is selected.

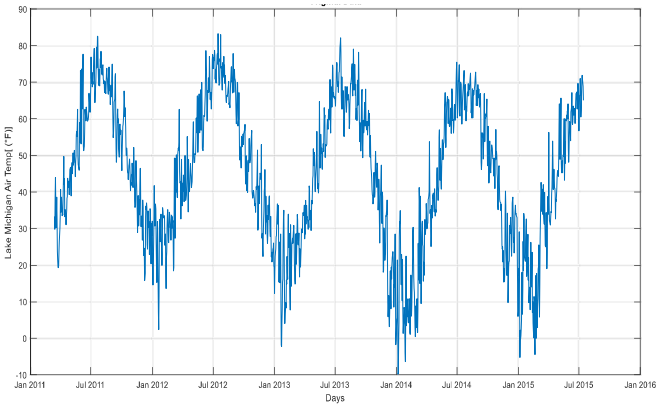

Figure 2: Daily mean air temperature of Michigan Great Lake

Corresponding entropy values are plotted for the different mother wavelets in figure 4.

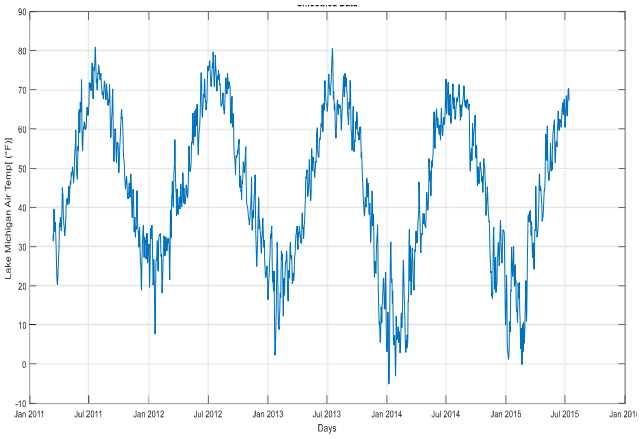

Figure 3: Exponentially smoothed data series

From figure 4, it is revealed that db2 and sym2 mother wavelets are the fittest for denoising the daily mean air temperature data series as they yield minimum entropy.

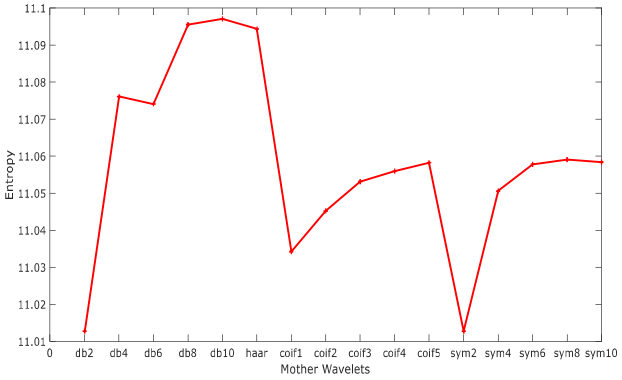

Figure 4: Entropy values for different mother wavelet

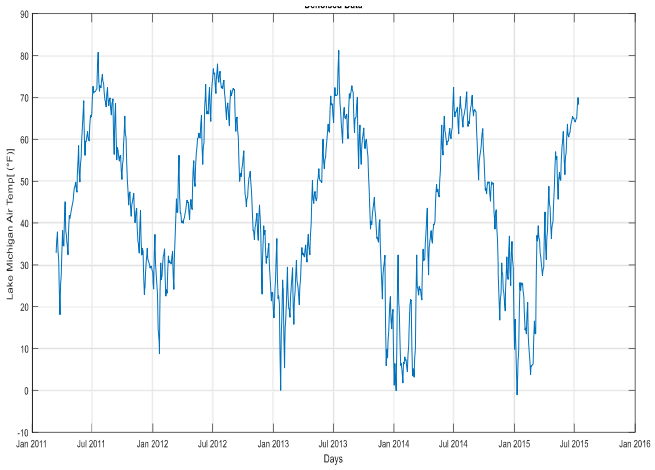

Figure 5: De-noised data series

The de-noised data using db2 as the mother wavelet is shown in figure 5.

In DVV scheme, the embedding dimension (m), [31] [32], embedding lag (τ) (Takens' embedding theorem [33]), RMSE and minimum target variance ($\sigma^{*2}_{\min}$) are evaluated and shown in table 1.

Table 1: Embedding dimension, lag, RMSE and $\sigma^{*2}_{\min}$ for test signal using DVV Scheme

Signal	Embedding dimension (m)	Embedding Lag (τ)	RMSE	$\sigma^{*2}_{\min}$
Air temperature signal over the Michigan Great Lake	4	64	0.105	0.1944

Figure 6 represents the DVV plot of the daily mean air temperature of the Michigan Great Lake from 14th March 2011 to 14th July 2015, whereas figure 7 shows the DVV Scatter plot for the same signal over the same duration. It is observed in figure 6 that the variance of the basic signal and the surrogate has a considerable mismatch between the trajectories. Furthermore, it is detected that the $\sigma^{*2}_{\min}$ is comparatively lower in the original test data series than the surrogate series. It indicates that the original signal is more deterministic than the surrogate signal.

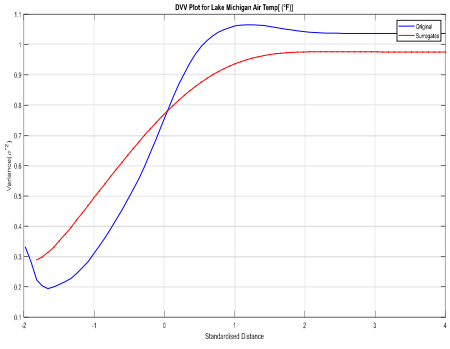

In figure 7, the DVV scatter diagram is plotted for the daily mean air temperature of the Michigan Great Lake. Both figure 6 and figure 7 advocate that the signal is non-linear. The deviation between the original and surrogate signal in figure 6 and the mismatch between the scatter diagram and the bisector line in figure 7 provide evidences in the favor of having considerable nonlinearity under test series.

The lowest tip of the DVV scatter plot diverges from the bisector line toward the vertical axis of the upper triangle in figure 7. This illustrates that the signal is deterministic.

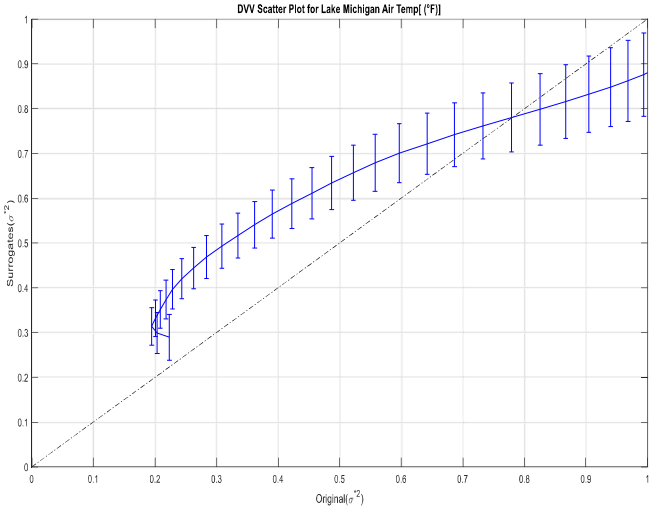

Figure 7: DVV Scatter diagram of Daily mean air temperature of the Michigan Great Lake.

IV. DISCUSSIONS & CONCLUSIONS

From Table 1, it is found that the value of the target variance $\sigma^{*2}_{\min}$ is low, which indicates the deterministic nature of the daily average air temperature variations of Michigan Great Lake. Therefore, predicting the future value of temperature can be done with significant reliability. The findings of the present research categories the current signal as non-linear, and deterministic. Numerous studies suggested that there exists interplay among temperature, precipitation, evaporation, snowfall, etc. [34] [35] [36] [37] [38] [39] [40] [41] [42] [43] [44]. This study's outcome could be useful for sectors like agriculture, fishing, tourism, industries, etc., around Lake Michigan as far as water resources management and overall planning are concerned.

V. REFERENCES

1. J. Byakatonda, B. P. Parida, P. K. Kenabatho and D. B. Moalafhi, "Analysis of rainfall and temperature time series to detect long-term climatic trends and variability over semi-arid Botswana," J. Earth Syst. Sci., vol. 127, no. 25, pp. 1 - 20, 2018

2. B. N. K. Reddy, R. Venkatesan, K. K. Osuri, S. Mathew S, J. Kadiyam and K. J. Joseph, "Comparison of AMSR-2 wind speed and sea surface temperature with moored buoy observations over the northern Indian ocean," J. Earth Syst. Sci., no. 127, 2018.

3. A. C. Patricia, D. Angela, M. McIlquhamd, M. Sancheza, K. Geiba, C. Hedberga, J. Hupy, M. W. Watsone, M. Fuoco, E. R. Olson, R. B. Pierce, C. Stanier, R. Long, L. Valin, S. Conley and M. Smithj, "Impacts of lake breeze meteorology on ozone gradient observations along Lake Michigan shorelines in Wisconsin," Atmospheric Environment, vol. 269, pp. 1 - 17, 2022.

4. "NOAA Regional Collaboration," The United States Government, [Online]. Available: https://www.regions.noaa.gov/great-lakes/index.php/regional-statistics/#_ftn1.

5. P. Holly, P. A. Steven, M. J. Michael, J. C. Paul and F. L. Gary, "Temperature Influence on Commercial Lake Whitefish Harvest in Eastern Lake Michigan," Journal of Great Lakes Research, vol. 29, no. 2, pp. 296 - 300, 2003.

6. I. A. S, R. Rudra, T. Dickinson, and M. Ahmed, "Trend and Periodicity of Temperature Time Series in Ontario," *American Journal of Climate Change,* vol. 3, no. 3, pp. 1 - 18, 2014.

7. M. L. Brenda, R. C. Stephen, D. B. S and B. E. Anne, "Links between type E botulism outbreaks, lake levels, and surface water temperatures in Lake Michigan," Journal of Great Lakes Research, vol. 37, no. 1, pp. 86 - 91, 2011.

8. Q. H. Frank and S. E. Cynthia, "A Reconstruction of Lake Michigan–Huron Water Levels Derived fromTree Ring Chronologies for the Period 1600–1961," *Journal of Great Lakes Research,* vol. 32, no. 1, pp. 29-39, 2006.

9. A. C. Craig, G.-B. Bharath , E. J. Travis, L. W. Anthony, K. M. Dana, C. R. Alexander, B. A. Holly, S. M. Amanda and B. M. Justin, "Spatio-temporal November and March snowfall trends in the Lake Michigan region," *International Journal of Climatology,* vol. 32, no. 8, pp. 3250-3263, 2018.

10. R. J. Robert and C. M. C. Elen, "Time Series Analysis of 20 Years of Hourly Precipitation in Southwest Michigan," Journal of Great Lakes Research, vol. 29, no. 2, pp. 256-267, 2003.

11. C. E. SELLINGER, C. A. STOW, C. E. LAMON and S. S. QIAN, "Recent Water Level Declines in the Lake Michigan-Huron System," Environ. Sci. Technol., vol. 42, no. 2, pp. 367-373, 2008.

12. N. NEKOUEE, B. ATAIE-ASHTIANI and S. A. HAMIDI, "Uncertainty analysis of wind-wave predictions in Lake Michigan," China Ocean Eng, vol. 30, pp. 811-820, 2016.

13. E. Ostertagova and O. Ostertag, "'Forecasting Using Simple Exponential Smoothing Method'," Acta Electrotechnica et Informatica, vol. 12, no. 3, p. 62–66, 2012.

14. C. K. Chui, L. Montefusco and L. Puccio, Wavelets: Theory,Algorithms, and Applications., vol. 5, Academic Press, 1994, p. 627.

15. I. Daubechies, "Ten Lectures on Wavelets.," SIAM, pp. 341-357, 1992.

16. T. Gautama, D. P. Mandic and M. M. Van Hulle, "The delay vectror variance method for detecting determinism and nonlinearity in time series," Phys D, vol. 1903, no. 4, pp. 167-176, 2004.

17. K. M. Hossain, D. N. Ghosh, K. Ghosh and A. K. Bhattacharya, ""Nonlinearity and chaos in 8B solar neutrino flux signals from sudbury neutrino observatory"," Fractal, vol. 20, no. 1, pp. 17-32, 2012.

18. I. A. Syed , R. Rudra, D. Trevor and M. Ahmed, "Trend and Periodicity of Temperature Time Series in Ontario," American Journal of Climate Change, vol. 3, no. 3, pp. 272 - 288, 2014.

19. V. Jaksic, D. P. Mandic, K. Ryan, B. Basu and V. Pakrashi, "A comprehensive study of the delay vector variance method for quantification of nonlinearity in dynamical systems," Royal Society Open Science, pp. 1 - 24, 2016.

20. R. G. Brown and R. F. Meyer, "The fundamental theory of exponential smoothing," Operations Research, vol. 9, no. 5, pp. 673 - 685, 1961.

21. T. Sarkar, . R. Ray, M. H. Khondekar, K. Ghosh and S. Banerjee, "Chaos and periodicity in solar wind speed: cycle 23," *Astrophys Space Sci,* vol. 357, no. 128, p. 1:10, 2015.

22. E. Hoˇsˇt´alkov´a and A. Proch´azka, Wavelet Signal and Image denoising, Wellesley-Cambridge Press, 1996.

23. D. L. Donoho and I. M. Johnstone, "Ideal Spatial Adaptation by Wavelet Shrinkage," *Biometrika,* vol. 81, no. 3, pp. 425-455, 1994.

24. D. L. Donoho, "De-Noising via Soft-Thresholding Tech Rept 409. Statistics, Stanford.," Satistics, Stanford, 1992.

25. P. Goel and B. Vidakovic, "Wavelet Transformations As Diversity Enhancers," *Duke University,* p. 21, 1995.

26. K. Gabriel and B. Vidakovic , "The partitioning of attached and detached eddy motion in the atmospheric surface layer using Lorentz wavelet filtering," *Boundary-Layer Meteorology,* vol. 77, pp. 153 - 172, 1995.

27. D. L. Donoho and I. M. Johnstone, "Adapting to Unknown Smoothness via Wavelet Shrinkage," *Journal of the American Statistical Association,* vol. 90, no. 432, pp. 1200-1224, 1995.

28. M. H. Khondekar, D. N. Ghosh, K. Ghosh and T. Saha, "Application of Signal Processing to Investigate the Total Active 8B Solar Neutrino Flux Signal from Sudbury Neutrino Observatory (SNO)," International Journal of Electronic Engineering Research, vol. 2, no. 3, pp. 303 - 324, 2010.

29. M. H. Khondekar, D. N. Ghosh, K. Ghosh and A. K. Bhattarcharya, "Nonlinearity and Chaos in 8B Solar Neutrino Flux Signals from Sudbury Neutrino Observatory," vol. 20, no. 1, p. 17:32, 2012.

30. D. Kugiumtzis, "Test your surrogate data before you test for nonlinearity," Phys.Rev. E, vol. 60, no. 3, pp. 2808-2816, 1999.

31. T. Gautama, M. M. V. Hulle and D. P. Mandic, "On the Characterisation of the Deterministic/Stochastic and Linear/ Nonlinear Nature of Time Series," 2004a.

32. T. Gautama, D. P. Mandic and M. M. Van Hulle, "The delay vectror variance method for detecting determinism and nonlinearity in time series," Phys. D, vol. 1903, no. 4, pp. 167-176, 2004b.

33. F. Takens, "Detecting strange attractors in turbulance," Dynam. Syst, 1980.

34. L. D. John, "Long-term Trends in the Seasonal Cycle of Great Lakes Water Levels," Journal of Great Lakes Research, vol. 27, no. 3, pp. 342-353, 2001.

35. C. P. Yee and M. R. D, "The 1987–89 drop in Great Lakes water levels, causes and effects. In: FitzGibbon," Bethesda, MD, USA, 1990.

36. M. M. J and F. G. L, "Recent climatic trends in nearshore water temperatures in the St. Lawrence Great Lakes," Limnology and Oceanography, vol. 44, no. 3, pp. 530-540, 1999.

37. M. Linda , H. Henry , L. Murray , W. Lisa , L. Brent , Q. Frank and S. Michel , "Climate Change Impacts on the Hydrology of the Great Lakes-St. Lawrence System," Canadian Water Resources Journal, vol. 25, no. 2, pp. 153-179, 2000.

38. L. M. Brent , Q. H. Frank, C. H. Anne , A. A. Raymond , E. J. Anthony and L. L. Carol, "Evaluation of Potential Impacts on Great Lakes Water Resources Based on Climate Scenarios of Two GCMs," Journal of Great Lakes Research, vol. 28, no. 4, pp. 537-554, 2002.

39. A. A. Raymond, Q. H. Frank and S. E. Cynthia, "Hydroclimatic Factors of the Recent Record Drop in Laurentian Great Lakes Water Levels," *Bulletin of the American Meteorological Society,* vol. 85, no. 8, p. 1143–1152, 2004.

40. M. E and M. H, "Assessment of impact of climate change on water resources: a long term analysis of the Great Lakes of," Hydrology and Earth System Sciences, vol. 12, no. 1, pp. 239-255, 2008.

41. H. L. Janel , K. V. Sergey and R. J. Paul, "Quasi-Periodic Decadal Cycles in Levels of Lakes Michigan and Huron," J. of Great Lakes Research, vol. 35, no. 1, pp. 30-35, 2009.

42. "Attribution of Decadal-Scale Lake-Level Trends in the Michigan-Huron System," *Water,* vol. 6, no. 8, p. 2278 – 2299, 2014.

43. S. C, B. D. P., H. N., F. V. and W. H., "Evaporation from Lake Superior: 2: Spatial distribution and variability," Journal of Great Lakes Research, vol. 37, no. 4, pp. 717-724, 2011.

44. A. D. Gronewold, B. J, D. D, S. J. P, C. A. H, S. F, Q. S. S, H. S. T and F. V, "Hydrological drivers of record-setting water level rise on Earth's largest lake system," Water Resources Research, vol. 52, no. 5, 2016.